Revisiting the latent heating contribution to foehn warming – Lagrangian analysis of two foehn events over the Swiss Alps

Annette K. Miltenberger[a b *], Silvia Reynolds[a c], Michael Sprenger[a]

[a] Institute for Atmospheric and Climate Science, ETH Zurich, Switzerland

[b] now at: Institute for Climate and Atmospheric Science, University of Leeds, United Kingdom

[c] now at: Office of Meteorology and Climatology MeteoSwiss, Federal Department of Home Affairs, Zurich, Switzerland

*Correspondence to: Annette K. Miltenberger (a.miltenberger@leeds.ac.uk)

Foehn flows are typically associated with quite warm air temperatures. Though several theories for the so-called foehn air warming have been developed over the past century, no conclusion about the most important mechanism has been reached. The development of new methods to calculate accurate air mass trajectories also over complex topography has opened up a new perspective on this question. Air mass trajectories derived wind field data from COSMO-model simulations with 20 s temporal resolution are used in this study to investigate the origin of the foehn air and the contribution of adiabatic and diabatic processes for two foehn events in the Swiss Alps with a focus on the Rhine valley. The first investigated foehn event has no precipitation on the upstream side of the Alps. The majority of air parcels stem from upstream altitudes above 1.8 km and most of the foehn air warming is due to adiabatic descent (∼ 79 %). In the second investigated event significant upstream precipitation occurred. For this case a significantly larger fraction of the foehn air parcels originate within the lowest 2 km of the upstream atmosphere (up to 70 %). Adiabatic descent accounts for the largest part of the temperature change (∼ 70 %), while moist-diabatic processes explain about 60 % of the potential temperature change. The vertical displacement across the Alpine range is correlated with the diabatic temperature change: parcels strongly heated by condensation, deposition and freezing are in general found at high altitudes above the foehn valley, while parcels affected by diabatic cooling through evaporation, sublimation and melting arrive closer to the valley floor. The high-resolution trajectories also indicate a much more complicated vertical and horizontal flow pattern than generally assumed with several distinct air streams upstream of the mountain range and vertical "scrambling" of air masses.

Key Words: foehn flow, foehn air warming, trajectories, ...

Received ...

1. Introduction

Foehn flows are a common feature of mountain meteorology, although disguised by different names, e.g., south and north foehn in the Alps, bora in the Dinaric Alps, chinook in the Rocky mountains, or Puelche and Raco in the Andes (Richner and Hächler 2013). South foehn in the northern Alpine valleys, the target area of this study, has a characteristic signal in surface observations typical of foehn winds in general: strong gusty winds go along with a substantial increase in temperature and decrease in relative humidity. The changes can be very abrupt, indicating that the foehn flow is already established at higher levels and suddenly touches down to the ground. The societal and economic impacts of these strong winds are well known: enhanced fire risks, impacts on air quality, beneficial impacts on agriculture, direct wind-driven damage to buildings and infrastructure, and human well-being (Richner and Hächler 2013).

Given its fierce nature, foehn flows have attracted the interest of researchers for a long time. The scientific foehn research started in the late 19th century with the aim to explain the ends of the ice ages (Heer and von der Linth 1852; Dove 1867). Hence, one key topic of this research was the origin of the warm foehn air masses. The first scientific ideas proposed a Saharan origin of the air arriving in the northern Alpine valleys (Heer and von der Linth 1852), an idea which was questioned by Dove (1867) who located the source region in the warm Caribbean Sea. In contrast to this foehn theory based on advection of warm air from 'remote' places, a localised theory was proposed by Hann (1866, 1885), which became known as the so-called thermodynamic foehn theory (Fig. 1a): air impinging on the southern Alpine slope is forced to rise along the obstacle, leading to substantial precipitation and hence latent heat release of the ascending air

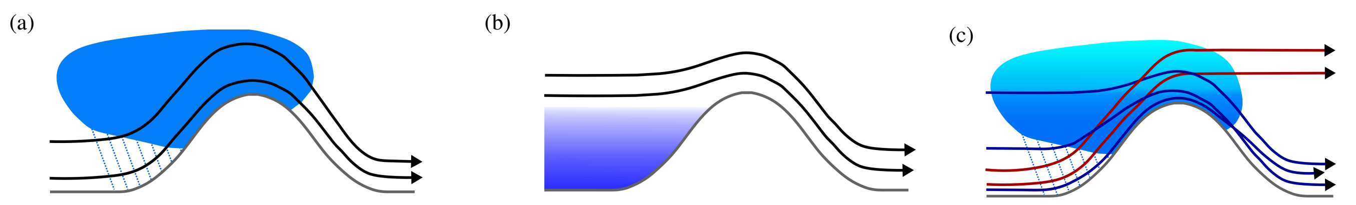

Figure 1. Illustration of the Swiss (thermodynamic) (a) and the Austrian foehn theory (b). In the thermodynamic foehn theory moist air is assumed to ascend over the upstream slope and to cool according to the moist-adiabatic lapse rate. Due to (heavy) precipitation on the upstream side, the air masses are assumed to be much drier once they reach the lee-side slope, where they descend and warm dry-adiabatically. In contrast, the Austrian foehn theory does not rely on the co-occurrence of warm temperatures in the foehn valley and upstream precipitation. The warm temperatures are explained by dry-adiabatic descent of air from above a stable, blocked air mass on the upstream side. (c) Illustration of the typical foehn trajectories from the foehn case with significant precipitation investigated in this study (May 2013). Parcels strongly heated by diabatic processes (condensation, deposition or freezing of water; red lines) remain at high altitudes on the lee side. In contrast, parcels affected by latent cooling (evaporation, sublimation or melting of hydrometeors; blue lines) descend into the foehn valleys on the lee side.

parcels. As soon as the air parcels reach the Alpine ridge, or north-south valley transects, and the remaining hydrometeors have evaporated, the moist-adiabatic ascent is followed by a dry-adiabatic descent into the northern valleys. The difference in the two lapse rates then explains, according to this theory, the temperature increase of the foehn air. To be more precise, this theory attempts to explain why the potential temperature of air parcels in the northern valleys are often higher than the ones on the Alpine south side. As intuitive as the theory appears, some substantial deficiencies could be identified. Seibert (1990, 2004, 2005) outlined the main problems concisely, e.g., by assessing that the amount of precipitation needed to explain the north-south difference in potential temperature is unrealistically high. Furthermore, there are even foehn events in the northern Alpine valleys which completely lack precipitation on the Alpine south side. Elvidge and Renfrew (2015) very concisely discussed further mechanisms, which may contribute to foehn warming. In particular, the foehn air might originate from higher altitudes, possibly due to low-level orographic blocking on the upwind side. The potentially warmer and dryer air at these levels then flows into the foehn valleys in an 'isentropic drawdown'. A range of studies has demonstrated the importance of this mechanism for several mountain ranges including the Alps, Iceland and Antarctica (e.g., Seibert 1990; Olafsson 2005; Elvidge *et al.* 2014; Grosvenor *et al.* 2014; Würsch and Sprenger 2015). Another mechanism mentioned by Elvidge and Renfrew (2015) is turbulent sensible heating and drying of the low-level flow due to mechanical mixing in a stably stratified atmosphere. This mechanism gained only little interest so far in relation to the foehn air warming problem. Finally, foehn flows are typically associated with dry, cloud-free conditions (but see Richner and Duerr, 2015, for the special conditions during dimmer foehn). Hence, the warming might also be due to direct radiative heating of low-level air on the lee side. In short, a unifying theory of foehn air warming remains elusive.

Part of the problem might be that a unifying theory does not exist at all. For instance, Hann (1866) already distinguished between different foehn types. His notation, the two foehn types I and II, is nowadays replaced by the 'Austrian' and 'Swiss' foehn types (Steinacker 2006). The geographical connotation already indicates where the two types are predominant, however, without precluding them to occur elsewhere. Recently, Würsch and Sprenger (2015) confirmed the different mean behaviour in the two regions with a trajectory analysis for the period 2000–2002. Air reaching a Swiss station ascended upwind of the Alps consistent with the thermodynamic theory. In contrast, air reaching an Austrian stations originated at higher altitudes above an inversion layer in the Po valley and descended dry-adiabatically into the foehn valleys (isentropic drawdown).

Trajectories have long-since been recognised as a powerful method to investigate the question of foehn warming (Richner and Hächler 2013) and questions of mountain meteorology in general (Chen and Smith 1987; Kljun *et al.* 2001; Roch 2011). However, the technical challenges are substantial due to the complex topography and the high temporal variability (gustiness) of the winds. Therefore, Würsch and Sprenger (2015) refrained from addressing this problem, given a relatively coarse horizontal grid spacing (7 km) and 1 h temporal resolution of the wind fields. Similar limitations apply to earlier Lagrangian studies assessing the source region of foehn air (e.g., Seibert *et al.* 2000). Indeed, it is illuminating that Elvidge and Renfrew (2015) proposed the Antarctic Peninsula as 'an ideal natural laboratory' for the study of foehn! There, the topography and the upstream conditions are often less intricate than for the Alps.

State-of-the-art high-resolution numerical models at least partly resolve the high spatial and temporal variability of the wind fields typical for mountainous terrain (e.g., Doyle *et al.* 2013). The coarse temporal resolution of the wind field data typically used for trajectory calculations prevents one from taking full advantage of these models for a Lagrangian analysis. Therefore online trajectory tools, which run parallel to the Eulerian simulation, are a major step forward in Lagrangian mountain meteorology. For instance, Miltenberger *et al.* (2013) implemented online trajectories into the COSMO model, hence allowing the trajectories to take full advantage of a 20 s time step. They applied the new method particularly to problems in orographic precipitation (Miltenberger *et al.* 2015), but an illustrative case of a north foehn study clearly showed the potential of the new method for foehn-related studies (Miltenberger 2014). In a systematic study, Bowman *et al.* (2013) looked at the minimal time resolution of the input winds required in Lagrangian models. They recommend a time step of 30 min for a 10 km grid spacing. Extrapolating this, a COSMO simulation with a 2 km resolution would need at least a 6 min time interval for the input wind - which in turn requires huge storage capacities and transmission bandwidths. While increasing the time resolution of the input wind fields will substantially reduce interpolation errors in the trajectory calculation, it will not eliminate errors in the wind fields themselves (Bowman *et al.* 2013). For instance, the representation of subgrid-scale turbulence most likely affects how the foehn winds are established and how far they descend into the foehn valleys (e.g., Gohm *et al.* 2008 for bora winds). This uncertainty cannot easily be resolved and puts some basic limitations on the representation of foehn winds in state-of-the-art NWP models and consequently in trajectory data sets (e.g., Wilhelm 2012 or a systematic study on foehn in COSMO during three years).

Trajectories in a turbulent flows require a cautious interpretation. Air mass trajectories, such as implemented by Miltenberger *et al.* (2013), do not represent the paths of individual air *particles* in the turbulent flow, but necessarily represent larger air *parcels*, with particle fluxes in and out of the air parcel's boundaries (Batchelor

1967for a detailed discussion of the air parcel concept). The time-mean effect of sub-grid processes such as turbulent mixing are represented as physical tendencies in otherwise conserved properties such as mass or energy along air mass trajectories (e.g., Stevens *et al.* 1996; Sodemann *et al.* 2008).

Despite these limitations of trajectories, the question of foehn air warming very recently gained new impetus from Lagrangian studies. Backward trajectories were used in two studies to investigate foehn air warming in the Toyama Plain (Japan). Ishizaki and Takayabu (2009) found dry- and moist-adiabatic processes as well as radiative heating to be important using wind field data from a climate model with 20 km grid spacing. With a Lagrangian energy budget analysis Takane and Kusaka (2011) showed that water vapour condensation did not contribute to record-high surface temperatures in the Tokyo area, but instead sensible heat fluxes from the surface played the most important role. A Lagrangian approach was also taken by Elvidge *et al.* (2014, 2015) to study warm foehn jets over the Larsen C Ice Shelf, Antarctica, and their influence on ice melting. In three different cases exhibiting varying degrees of flow linearity, the foehn jets are identified as manifestations of gap flows. The backward trajectory analysis traces the cool and moist conditions within the foehn jets as compared to the background wake to different source regions and a reduced diabatic warming. Finally, an interesting hypothesis was proposed by Smith *et al.* (2003) based on a small sample of trajectories for a south foehn case: air parcels ascending on the Alpine south side and producing precipitation continue to rise on the lee side, while trajectories descending into the foehn valley gain little heat by diabatic processes. Hence, in their words "parcels with different heating histories ascend or descend to reach their buoyant equilibrium". They suggested that the scrambling of air parcels should be included in future conceptual models of air mass transformations, and in foehn dynamics in particular.

These new studies show that the old-standing problem of foehn warming can be addressed anew and potentially brought forward based on Lagrangian methods. The aim of the present study fits in very nicely with this new perspective. Its very specific research questions are to

1. analyse the horizontal and vertical pathway of air arriving in the Rhine valley,
2. quantify the foehn warming due to isentropic drawdown and microphysical processes in the Swiss Rhine valley, and
3. decompose the moist-adiabatic contribution into several different microphysical processes.

Note that the study does *not* explicitly quantify the warming effect due to turbulent mixing and radiative heating (or other non-microphysical processes), and hence does not intend to consider the warming problem exhaustively. However, the focus on different microphysical processes will allow unexpected compensating effects to be discussed.

The research questions listed above are addressed by considering two different foehn cases in 2013: one lacking upstream precipitation (4-7 March 2013, dry foehn event) and one with substantial upstream precipitation (14-16 May 2013, moist foehn event). The comparison of the two cases will allow us to asses the warming mechanisms in two potentially very different situations. The analysis presented in this study is restricted to the upper Rhine valley, a major foehn valley between Switzerland and Austria. This area was a target area in the Mesoscale Alpine Programme (MAP, Bougeault *et al.* 2001), an international field experiment with intense observation periods in September 1999. The sub-project FORM within MAP explicitly addressed the foehn in the Rhine valley (Richner *et al.* 2006; Drobinski *et al.* 2007). Further studies focussing on foehn in the Rhine valley considered the foehn's influence on the ozone distribution (Baumann *et al.* 2001), investigated the important interaction of the foehn flow with the cold-air pools (Flamant *et al.* 2006), presented wind profiler measurements (Vogt and Jaubert 2004), and performed numerical simulations of a foehn event (Zängl *et al.* 2004). In short, the two cases selected for this study fit in nicely with the already existing literature about the foehn flow in one of the best studied foehn valleys in the Alps.

The remainder of the article is structured as follows: section 2 describes the weather prediction model, the trajectory calculation and the diagnostics used. Section 3 presents the dry foehn event, followed by the moist foehn event in section 4. Finally, section 5 summarises the main results.

2. Numerical model data and diagnostics

2.1. Model Set-Up and Trajectory Data

The foehn cases were modeled with the non-hydrostatic numerical weather prediction model COSMO (version 4.7) (Baldauf *et al.* 2011). All simulations were conducted with a horizontal grid spacing of 2.2 km (COSMO-2). Boundary and initial conditions are derived from a COSMO-model simulation with a horizontal grid spacing of 7 km driven by ERA-Interim data (Dee *et al.* 2011). The COSMO-2 domain covers the greater Alpine region (approximately 41–50° N and 1–17° E). 60 levels with a mean spacing of 388 m were used (13 m close to the surface and 1190 m at 23 km). No parameterisation of deep convection was employed for the COSMO-2 simulations, while COSMO-7 used the Tiedtke scheme. Cloud microphysical processes were parameterised with the two-moment scheme of Seifert and Beheng (2006), which predicts mass and number densities of five hydrometeor classes (cloud, rain, ice, snow and graupel). Finally, boundary-layer, surface and turbulent processes were all parameterised (Raschendorfer 2001; Baldauf *et al.* 2011). The COSMO-2 simulation starts at 21 UTC 3 March 2013 for the dry foehn case and at 03 UTC 14 May 2013 for the moist foehn case. The simulations were run for 102 and 93 hours, respectively.

The Lagrangian analysis is based on trajectories calculated with the new online-trajectory module (Miltenberger *et al.* 2013). It solves the trajectory equation using the grid-scale wind field at each Eulerian model timestep (20 s). The wind field at the trajectory location is calculated from the neighbouring eight grid points by trilinear spatial interpolation along the model coordinate system.

Forward trajectories were started every 0.02°(about 2 km) along a line over Northern Italy (approximately between 43° N, 6° E and 45° N, 17° E). In the vertical, starting points were located every 100 m between the surface and 4 km altitude. Trajectories were started every hour between 23 UTC 3 March 2013 and 00 UTC 6 March 2013 for the dry case, and between 05 UTC 14 May 2013 and 08 UTC 16 May 2013 for the moist case. For further analysis we considered only trajectories passing through the Rhine valley, which we defined as a rectangular box with an extent of 0.58°× 1.05°centred at 47.16°N, 9.53°E (green box in Fig. 3b). Additionally, for the dry case only, trajectories had to stay outside clouds, hence being representative of the first dry episode. Figure 2 (grey points) shows when and at which altitude the air parcels arrive in the Rhine valley. For both foehn cases, many air parcels are found in the lowest 3 km above the valley floor, i.e., the valley atmosphere. In total **14125** (27491) trajectories are included in the analysis for the dry (moist) foehn event.

The air parcels' history is studied based on the following variables, all being available at 20 s temporal resolution: air temperature, pressure, the mixing ratio of water vapour, cloud droplets, rain, ice, graupel and snow, and the three velocity components. For the moist case, additionally, all microphysical rates involving phase changes of water were studied. In accordance with the trajectory calculation, the variables have been derived by trilinear spatial interpolation from the Eulerian fields.

2.2. *Variables and Diagnostics*

For adiabatic, frictionless flow the potential temperature θ is conserved along air mass trajectories. If diabatic processes occur, potential temperature changes according to

$$\frac{D\theta}{Dt} = S_{lh} + S_{rad} + S_{turb} \tag{1}$$

where S_{lh} denotes the impact of latent heating, S_{rad} of long- and short-wave radiation and S_{turb} of turbulence (including diffusion in a numerical model). The term S_{lh} depends on cloud microphysical processes and can be further decomposed into

$$S_{lh} = S_{dep} + S_{cond} + S_{freez} - S_{sub} - S_{evap} - S_{melt} \tag{2}$$

where the terms describe the change due to vapour deposition on frozen hydrometeors (S_{dep}), condensation on liquid hydrometeors (S_{cond}), freezing of liquid hydrometeors including riming (S_{freez}), sublimation of frozen hydrometeors (S_{sub}), evaporation of liquid hydrometeors (S_{evap}) and melting of frozen hydrometeors (S_{melt}).
The latent heating rates S_x, where x stands for any of the six processes listed above, are calculated according to

$$S_x(t) \approx \frac{DT}{Dt}|_x \left(\frac{p_0}{p}\right)^{R/c_p} = \frac{L_q}{c_p}\frac{Dq}{Dt}|_x \left(\frac{p_0}{p}\right)^{R/c_p} \tag{3}$$

where q is the mass mixing ratio of the relevant hydrometeor category for process x, e.g., cloud and rain water content for evaporation and ice, snow and graupel water content for melting. L_q is the latent heat of phase change, c_p the heat capacity of air and R the gas constant of air. Note that this approach assumes that pressure changes due to microphysical processes are negligible. But with this restriction, the approach allows us to quantify the role of different microphysical processes for the net latent heating along trajectories. Of particular interest will be the latent heating between a location upstream of the Alpine ridge (45°N, green dashed line labelled “upstream” in Fig. 3b) and one in the Rhine valley (“ALT” in Fig. 3b).
Finally, some remarks concerning numerical artefacts are necessary. Potential temperature is perfectly conserved along trajectories in an adiabatic, frictionless flow. However, this does not necessarily apply for numerically computed trajectories, because (i) conservation might be affected by numerical approximations to the trajectory equation (truncation and interpolation errors) and (ii) numerical diffusion and non-conservative advection in the NWP model might introduce artificial changes in potential temperature (e.g., Stohl and Seibert 1998). The magnitude of these effects can only be assessed in a budget closure study, i.e., each term in eq. 1 must be explicitly quantified. Unfortunately, not all required terms are available for the current study. However, previous studies indicate that the trajectories significantly improve with increasing temporal resolution of the input wind fields (e.g., Stohl and Seibert 1998; Grell *et al.* 2004; Bowman *et al.* 2013). Since the focus of our study is on latent heating, any numerical artefacts in the potential temperature budget will be contained in $\Delta\theta$ for the dry case and $\Delta\theta - S_{lh}$ for the moist case, respectively.

3. Dry foehn event

3.1. *Synoptic situation*

A long-lasting south foehn event was observed in the Rhine valley during the period 4-7 March 2013. At its beginning, an upper-level trough, located off the coast of Portugal, steered warm southerly air towards the Alps. As this trough moved further eastward, a strong pressure gradient developed across the Alps resulting in a pronounced foehn knee in the sea-level pressure field (contour lines in Fig. 3a). Streaks of high wind velocity emanating from the northern Alpine foehn valleys are visible in the low-level wind fields and a strong low-level jet developed on the western side of the Alps (colour shading in Fig. 3a). During the first 20 h of the foehn event no precipitation was observed on the southern side of the Alps, which is well reproduced in the model simulations (Fig. 3b). In contrast, the second phase of the foehn event on 6 March 2013 is characterised by transient heavy precipitation (not shown). Finally, during the night of 6 to 7 March 2013 the low-pressure system associated with the upper-level trough dissolved and subsequently the foehn flow ceased in the Rhine valley. More specifically, the foehn started at 22 UTC 4 March 2013 in the Rhine valley (in Vaduz) and foehn conditions lasted until 5 UTC 7 March 2013 (Arbeitsgemeinschaft Föhnforschung Rheintal-Bodensee 2014).
At the surface weather station in Vaduz the onset of the foehn event was marked by a strong increase in temperature of 13 K and a drop in relative humidity of 60 % (cyan and red lines in Fig. 2a). While the foehn flow at upper levels develops within our COSMO-2 simulation, the rapid increase of potential temperature and wind speed in the Rhine valley is not captured at ground level. High wind speeds and warm temperatures associated with the foehn flow remain several hundred meters above model ground level (not shown), indicating that the foehn flow is not able to penetrate further towards the surface in the model. The timing of the foehn flow at higher levels and the onset of upstream precipitation is well simulated by COSMO-2. In the following, only the first dry phase of the foehn event between 22 UTC 4 March and 18 UTC 5 March will be further analysed. Due to the lack of any significant upstream precipitation microphysical processes can be neglected during this phase.

3.2. *Origin of foehn air*

Two different sources of the foehn air can be identified during almost the entire first period of the foehn event. One trajectory bundle originating over western Italy and one including trajectories originating further east towards the Adriatic sea (Fig. 4). Trajectories in the first bundle follow an almost straight north-south line across the Alps. Upstream of the Alps these air parcels are located at altitudes larger than 1.8 km over the Po valley and they ascend only very little on their approach to the Alpine range (on average about 300 m, Fig. 4). In contrast, trajectories from the second bundle have a more northwesterly direction south of the Alps and are located at slightly lower levels around 1.5 km. A closer analysis of the upstream conditions indicates that these trajectories originate from a thin filament at the top of the planetary boundary layer, which stretches over the entire Po valley. The lower level branch is absent in the first hours of the foehn event, but later contributes between 20 % and 40 % of all foehn trajectories. On the northern side of the Alps trajectories from both air streams descend rapidly (Fig. 4). Above the central Rhine valley the air parcels are, on average, at about the same altitude as on the southern side. Further downstream (Altstätten), they have reached a level about 700 m below their upstream altitude. Trajectories with the furthest descent have altitudes between 1.5–2.0 km above Altstätten,

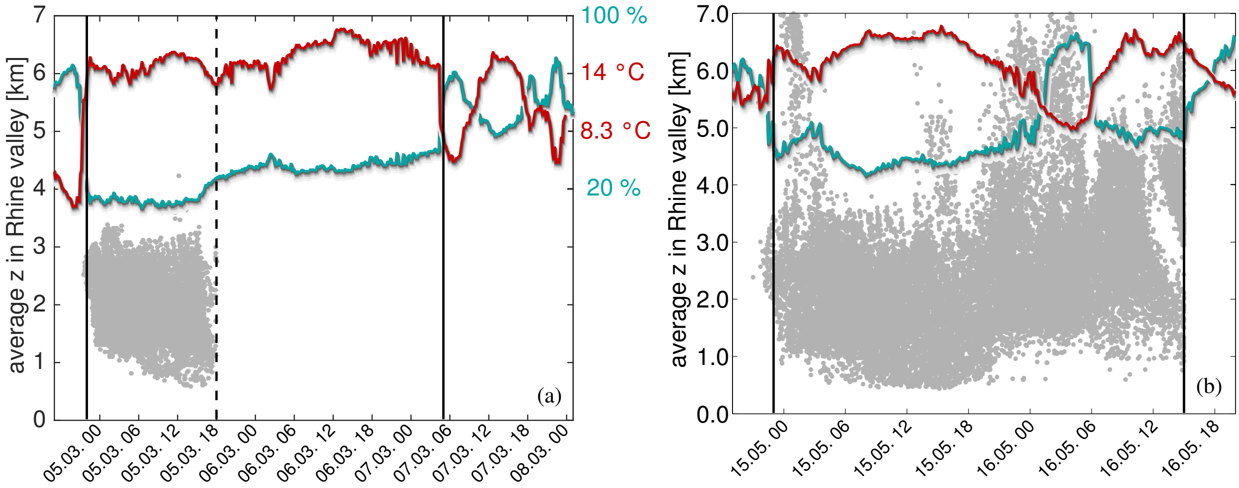

Figure 2. Height-time distribution of the trajectories (grey dots) passing over the Rhine valley (defined by the green box in Fig. 3b) for the March (a) and the May 2013 (b) event. Additionally, the evolution of the 2 m air temperature (red) and relative humidity (cyan, units on the right) at the SwissMetNet station in Vaduz is displayed. The left vertical black line indicates the onset of foehn in Vaduz and the right one its cessation according to the AGF data base (Arbeitsgemeinschaft Föhnforschung Rheintal-Bodensee 2014). The black dashed line in panel (a) indicates the onset of significant surface precipitation over the southern slopes of the Alps.

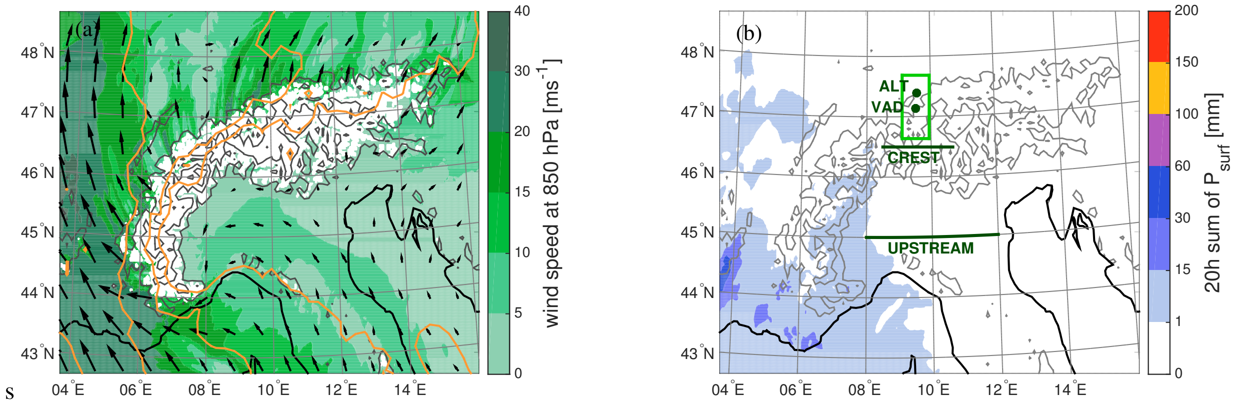

Figure 3. Dry foehn case: synoptic scale conditions. (a) Horizontal wind field at 850 hPa (colour shading) and mean sea level pressure (orange lines, contour intervals of 5 hPa) on 08 UTC 05 March 2013. (b) Accumulated surface precipitation for the period between 22 UTC 04 March and 18 UTC 05 March 2013. The green box indicates the area used for the selection of the trajectories. Several important locations for the evaluation of the trajectory data are indicated: the air parcels' upstream properties are retrieved along the line labelled "upstream" and their properties above the highest topography at the line labelled "crest". In addition, the location of Vaduz (VAD) and Altstätten (ALT) in the Rhine valley are shown, which are used to determine the air parcels' properties within the foehn valley. Grey contours in both panels show the topography (contour intervals of 1 km).

which coincides with a location of strong warming in COSMO-2 cross-sections along the Rhine valley (not shown). The furthest descent is observed at the beginning of the foehn event. In the late afternoon and the evening, i.e., immediately before and during the onset of upstream precipitation, the number of parcels experiencing a strong net downward displacement decreases and those experiencing a positive net vertical displacement increases (not shown).

3.3. Temperature and moisture budget

All air parcels experience substantial temperature changes (ΔT) during the passage of the Alpine ridge (Fig. 5b). Between their upstream location and the Alpine crest almost all parcels cool, in the mean by -4 $^\circ$C (red bars). After passing the crest, the temperature rises again resulting in a net temperature increase of about 6.5 $^\circ$C at Altstätten (cyan bars). For individual trajectories the south-north temperature change varies between -2 $^\circ$C and 15 $^\circ$C. In the first five hours of the foehn event trajectories passing the Rhine valley in the lowest 1.5 km of the atmosphere tend to warm more strongly than trajectories passing at higher levels, afterwards the relation is reversed (Fig. 5a). This is consistent with the warmest air being located between 1.5 and 2 km altitude in Eulerian cross-sections (sec. 3.1). The smallest ΔT values occur for all trajectories in the early morning hours between about 5 and 8 UTC.

Overall, the temperature change agrees very well with temperature changes expected as a results of the vertical parcel motion discussed in the previous section (isentropic drawdown): the parcel temperature decreases in regions of ascent (south of the Alpine crest), and rises during the descent north of the Alpine crest. For adiabatic flow, the potential temperature should not change along trajectories. At 0.24 K, the mean potential temperature change $\Delta\theta$ is indeed very close to 0 K during this dry phase of the foehn (Fig. 6a). The contribution of isentropic drawdown to the temperature change is quantified by the ratio of the adiabatic temperature change to the sum of the absolute adiabatic and diabatic one: $|\Delta T_{adia}|/(|\Delta T_{adia}| + |\Delta T_{diab}|)$. In this metric isentropic drawdown, on average, accounts for 78.6 % of the total temperature change (Fig. 5c). While there is little difference between parcels passing within the valley atmosphere (blue line) and above (cyan line), the importance of adiabatic processes steadily decline from almost 90 % to about 70 %

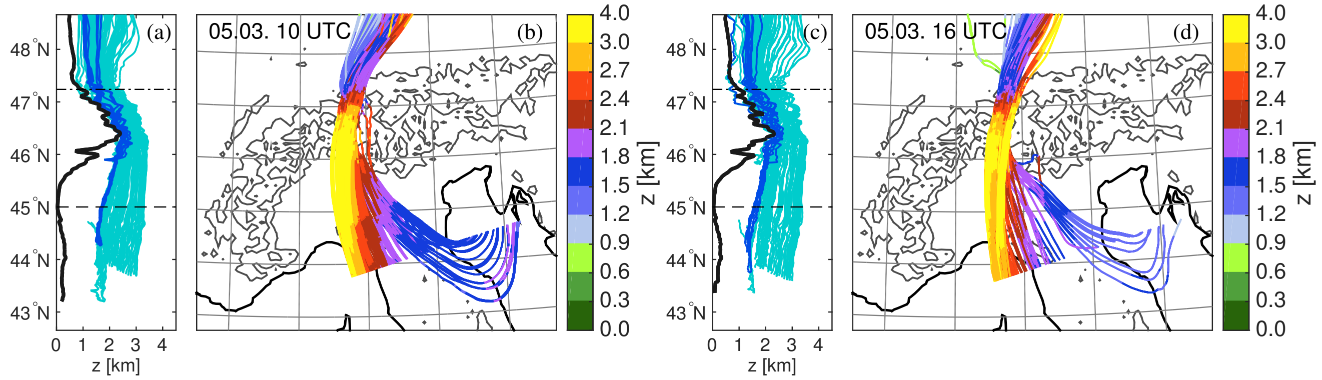

Figure 4. Dry foehn case: path of air parcels arriving in the Rhine valley in 20 min intervals centred around 10 UTC (a) and 16 UTC (b) on 05 March 2013. For both dates the path of the trajectories is shown in the height-latitude plane (a, c) and in the latitude-longitude plane (b, d). The color coding of the trajectories in the latitude-longitude plots indicates their altitude. Grey contours in both panels show the topography (contour intervals of 1 km). In the height-latitude plots trajectories with upstream altitudes (altitude at 45°N) below 1.7 km are shown in dark blue and those with larger upstream altitudes in cyan. The black line indicates the mean topography beneath the trajectories.

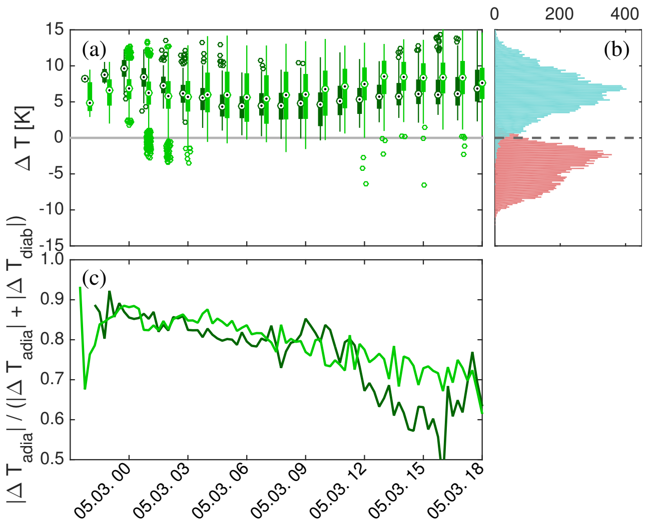

Figure 5. Dry foehn case: temperature change ΔT along trajectories between their upstream location and Altstätten (s. definitions in Fig. 3). (a) ΔT as a function of the trajectory arrival time in Altstätten. Values for trajectories within the valley atmosphere, i.e., below 1.5 km above Altstätten, are shown in dark green and those for trajectories passing higher up in light green. The black dot represents the median, the upper and lower ends of the bars the 25th and 75th percentile. Open circle show data points deviating by more than 2.7 standard deviations from the median. (b) Distribution of ΔT for all trajectories between the upstream location and the crest (red) or Altstätten (cyan). (c) Fraction of the potential temperature change explainable by adiabatic motion for parcels arriving below 1.5 km (dark green) and above (light green).

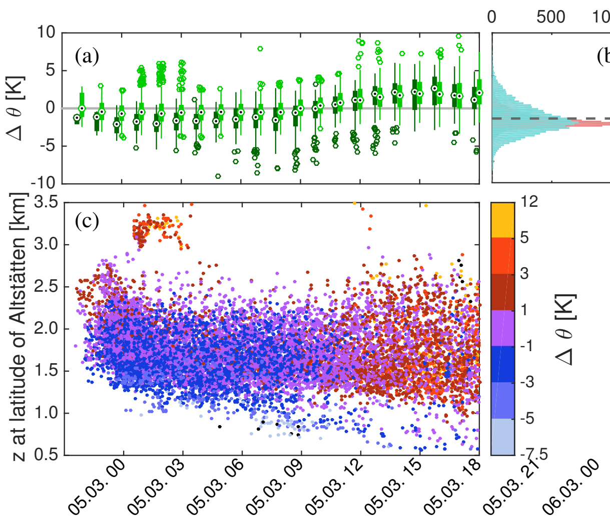

Figure 6. Dry foehn case: potential temperature change $\Delta\theta$ along trajectories between their upstream location and Altstätten (see definitions in Fig. 3). (a, b) are identical to those in Fig. 6 but pertain to potential temperature. (c) Each dot corresponds to a trajectory passing above 47.4°N at the corresponding time and altitude. The color coding corresponds to the $\Delta\theta$ between the upstream location and Altstätten.

percent. The non-adiabatic temperature change $\Delta\theta$ is only very weakly correlated with ΔT (R=-0.18). Values of $\Delta\theta$ vary between -5 K and 7 K for individual air parcels (Fig. 6a). The spread of the $\Delta\theta$ increases significantly over the downstream slope (red and cyan histograms). Differences between trajectories passing at different altitudes are small (Fig. 6a,c), but $\Delta\theta$ values depend on the arrival time in the Rhine valley. While negative potential temperature changes dominate before 10 UTC, the majority of parcels have positiveve $\Delta\theta$ afterwards (Fig. 6c). Turbulent mixing or radiative effects (eq. 1) must be responsible for the diabatic temperature changes, because warming due to microphysical processes can be ruled out in the period considered (Fig. 3a). Of course, other potential sources are violations of energy conservation in the numerical weather prediction model or the trajectory calculation (sec. 2.2).

Terrain-induced gravity waves or wind shear generated at the boundaries of the strongly accelerated foehn stream, mechanically enhances turbulent mixing. In accordance with this, Richardson numbers well below 1 and rather high values of turbulent kinetic energy are simulated by COSMO-2 on the downstream side of the Alpine range (not shown). Between the central and lower Rhine valley the $\Delta\theta$ distribution extends particularly towards colder values (not shown), which could be explicable by mixing with colder air close to the valley floor. In contrast, the diabatic temperature changes observed upstream of the Alps are more difficult to understand: there, the Richardson number is in general rather high and the turbulent kinetic energy small. However, most of the air parcels originate within a thin filament at the top of the planetary boundary layer and therefore may well be affected by mixing. Also, over the mountain ranges south of the crest, gravity waves form, which can enhance mixing mechanically. The temporal variation of $\Delta\theta$ also suggests an influence of radiative processes, as the potential temperature increases for trajectories travelling predominantly during daytime and decreases for those travelling during nighttime.

So far, only the temperature budget along the trajectories was considered. The moisture budget of the air parcels further supports our findings. The overall moisture change is very small (on average 0.3 g kg^{-1} up to the crest and 0.7 g kg^{-1} up to Altstätten, Fig. 7b). Hardly any trajectories lose moisture (Fig. 7b). The

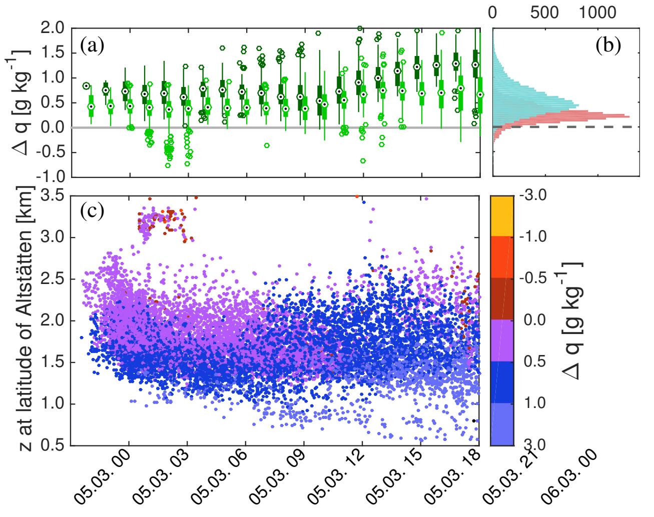

Figure 7. Dry foehn case: specific moisture change Δq along trajectories between their upstream location and Altstätten (see definitions in Fig. 3). (a, b) are identical to those in Fig. 6 but pertain to specific humidity. (c) Each dot corresponds to a trajectory passing above 47.4°N at the corresponding time and altitude. The color coding corresponds to the Δq between the upstream location and Altstätten.

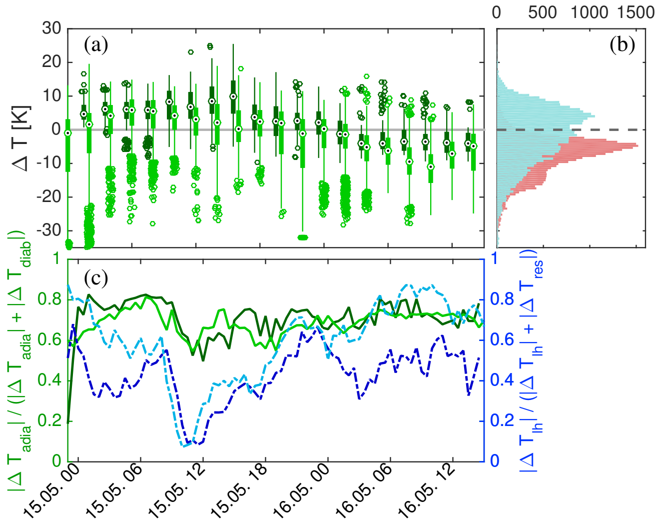

Figure 10. Moist foehn case: temperature change ΔT along trajectories between their upstream location and Altstätten (see definitions in Fig. 3). (a) ΔT as a function of the trajectory arrival time in Altstätten. Values for trajectories within the valley atmosphere, i.e., below 1.5 km above Altstätten, are shown in dark green and those for trajectories passing higher up in light green. (b) Distribution of ΔT for all trajectories between the upstream location and the crest (red) or Altstätten (cyan). (c) Fraction of the potential temperature change explicable by adiabatic motion for parcels arriving below 1.5 km (dark green) and above (light green).

moisture gain increases for all parcels after 9 UTC and it is in general larger for parcels passing at altitudes below 1.5 km through the Rhine valley (Fig. 7a,c). These observations are consistent with turbulent mixing with moist boundary layer air and the absence of precipitation formation, which would reduce the moisture content.

4. Moist foehn event

4.1. Synoptic situation

figure 9 The second foehn event analysed in this paper occurred between 14 and 16 May 2013. Strong southerly flow was steered towards the Alps on the downstream side of an extended upper-level trough associated with a surface low over the British Isles. Within this synoptic scale environment a strong pressure gradient developed across the Alpine range leading to foehn flow in the northern Alpine valleys and the formation of a strong low-level jet around the western side of the Alps (Fig. 8a). In contrast to the previous case, precipitation on the upstream side occurred during the entire foehn event with observed values locally exceeding 100 mm. The model precipitation of 60 to 100 mm agrees well with observed values (Fig. 8b). During the evening of 16 May the upper-level trough developed into a cut-off low to the west of France. With the related change in the large-scale flow direction foehn flow ceased.

In the Rhine valley foehn flow was established around 23 UTC 14 May and lasted until 15 UTC 16 May 2013 (Arbeitsgemeinschaft Föhnforschung Rheintal-Bodensee 2014). At the surface station Vaduz the foehn onset was marked by a strong increase in wind speed, a drop in relative humidity by about 30 % and a rise in air temperature by about 5 K (Fig. 2b). This foehn signal is somewhat smaller than in the previously discussed case (temperature increase 13 K, relative humidity drop 60 %). Foehn flow developed also in the COSMO-2 simulation leading to a marked increase in temperature and wind speed in the Rhine valley. In contrast to the previous case, the foehn flow in the model penetrates the entire valley atmosphere. However, the amplitude of the diurnal cycle is overestimated by about a factor two in the lowest 500 m. The timing of foehn onset and cessation agrees well with the observations.

4.2. Origin of foehn air

The source area of the foehn air mass shifts continuously eastwards throughout the foehn event from the Gulf of Genoa to the Adriatic Sea (Fig. 9). The upstream altitude of the parcels varies between several hundred meters and 3 km. Parcels with upstream altitudes below 1.7 km (low-level trajectories) originate further east than higher level parcels, at times forming two distinct air streams with different horizontal paths. A similar pattern emerged in the dry case. In the first phase of the event (until 12 UTC 15 May) low-level trajectories constitute about 40 % of all trajectories. Low-level trajectories ascend during their approach to the Alps, while high-level trajectories remain at almost constant altitude (Fig. 9a). Over the northern slope of the Alps high-level trajectories descend below 2.5 km, low-level trajectories descend more slowly. We refer to this pattern of vertical displacement as "scrambling" of air masses, as suggested earlier by Smith *et al.* (2003). At later stages the contribution of low-level trajectories to the foehn flow reaches 80 % (Fig. 9b), although the low-level air stream temporarily ceases during the night hours of 15 and 16 May. Consistent with the low source altitudes almost all parcels rise by several hundred meters over the southern Alps. However, the descent on the northern side is less pronounced and low-level trajectories pass the Rhine valley anywhere between the surface and 3 km altitude (Fig. 9b).

Over the entire foehn event the mean vertical displacement of parcels across the Alpine ridge is 0.46 km with values for individual parcels varying between -2 km and 5 km. While in the dry foehn case all trajectories showed a negative vertical displacement in the lower Rhine valley, in the moist case only 50 % of the parcels have a negative vertical displacement. The upstream ascent is on average larger (1.1 km compared to 0.4 km) and the downstream descent smaller (0.7 km compared to 1.1 km) than in the dry foehn case.

4.3. Temperature and moisture budget

The temperature of almost all air parcels decreases between their upstream location and the passage of the Alpine crest (on average: -8.3 °C, Fig. 10b red histogram). Between the upstream

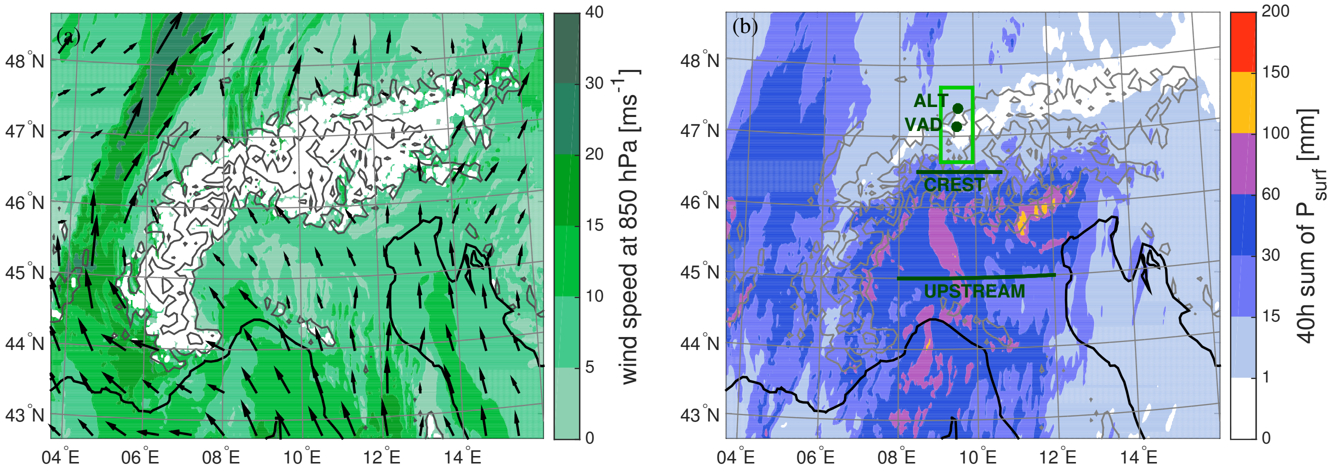

Figure 8. Moist foehn event: Synoptic scale conditions during the south foehn event in May 2013. (a) Horizontal wind field at 850 hPa and mean sea level pressure (orange lines, contour intervals of 5 hPa) on 12 UTC 15 May 2013. (b) Accumulated surface precipitation for the period between 23 UTC 14 May and 15 UTC 16 May 2013. Grey contours in both panels show the topography (contour intervals of 1 km).

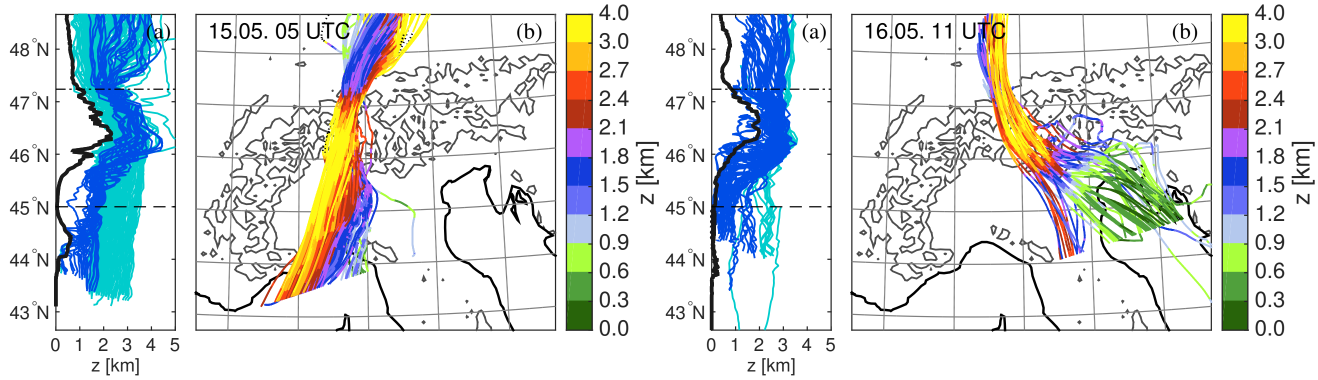

Figure 9. Moist foehn event: Path of the air parcels arriving in the Rhine valley in 20 min intervals centred around 05 UTC on 15 May 2013 (a) and 11 UTC on 16 May 2013 (b). For both dates the path of the trajectories is shown in the height-latitude plane (left) and in the latitude-longitude plane (right). The color coding of the trajectories in the latitude-longitude plots indicates their altitude. Grey contours in both panels show the topography (contour intervals of 1 km). In the height-latitude plots trajectories with upstream altitudes (altitude at 45°N) below 1.7 km are shown in dark blue and those with larger upstream altitudes in cyan. The black line indicates the mean topography beneath the trajectories.

location and Altstätten the temperature change ΔT of individual trajectories varies between -40 °C and 20 °C, where about 50 % of the trajectories experience a warming (Fig. 10b cyan histogram, mean: -1.8 °C). Overall this is consistent with the vertical displacements discussed in the previous section and hence points to the isentropic drawdown mechanism. Accordingly, between 60 % and 80 % of the temperature variation can be explained by adiabatic motion of the trajectories (Fig. 10c blue curves). This applies for both trajectories passing within the Rhine valley (solid blue line), i.e., with downstream altitudes less than 1.5 km, and trajectories passing aloft (dashed blue line). On average the temperature change for trajectories within the Rhine valley is slightly larger than for trajectories passing aloft (Fig. 10a). The difference is particularly pronounced between 12 UTC and 18 UTC 15 May and between 06 UTC and 12 UTC 16 May. In the first half of the foehn event the majority of trajectories undergo a warming, while cooling trajectories are more common during 16 May. During the second half of the foehn event hardly any foehn trajectories have upstream altitudes larger than 1.8 km, which makes it difficult for parcels to descend relative to their upstream altitude and thereby explains the decrease of the mean ΔT.

Consistent with the large contribution of adiabatic temperature changes, the potential temperature changes $\Delta\theta$ are smaller than ΔT: values for individual trajectories vary between -10 K and 20 K (Fig. 11b cyan histogram). For over 80 % of the trajectories

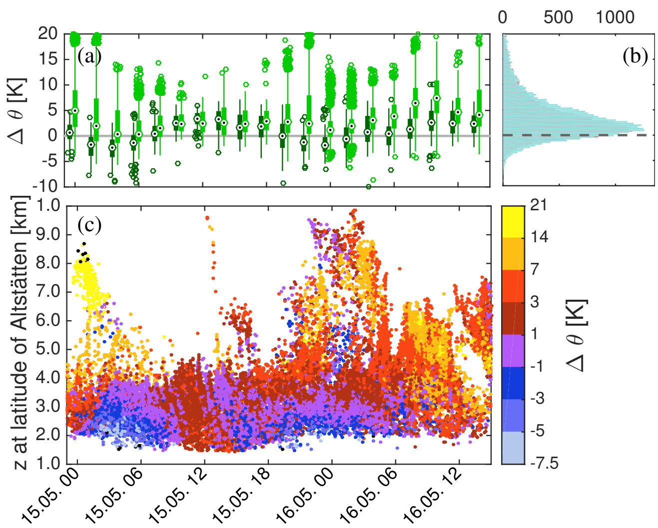

Figure 11. Moist foehn case: potential temperature change $\Delta\theta$ along trajectories between their upstream location and Altstätten (see definitions in Fig. 3). (a, b) are identical to those in Fig. 6 but pertain to potential temperature. (c) Each dot corresponds to a trajectory passing above 47.4°N at the corresponding time and altitude. The colour coding corresponds to the $\Delta\theta$ between the upstream location and Altstätten.

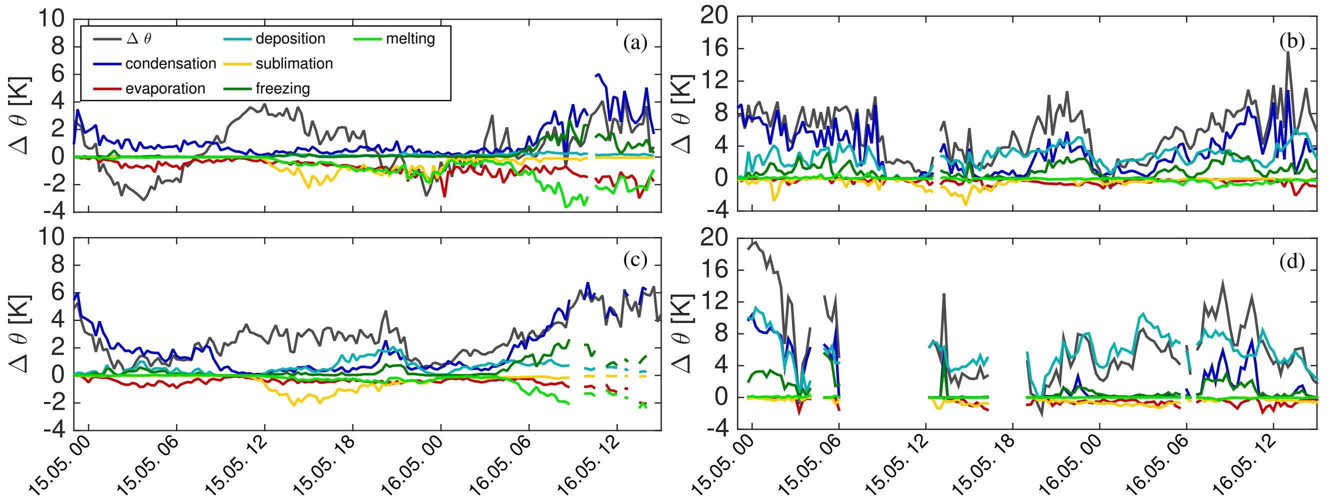

Figure 13. Moist foehn event: contribution of different microphysical processes to the net latent heating as a function of the trajectory arrival time in the Rhine valley: condensation (blue), evaporation (red), deposition (cyan), sublimation (yellow), freezing (dark green) and melting (light green). In addition, the net potential temperature change is shown (dark grey). The potential temperature changes were evaluated between 45°N and 47.4°N for each trajectory. The shown values are averages over those for individual trajectories arriving within 15 min intervals. Separate averages were computed for trajectories arriving below 1.5 km (a), between 1.5 km and 3.0 km (c), between 3.0 km and 4.5 km (b) and above 4.5 km (d).

the potential temperature increases with a mean $\Delta\theta$ of 3.4 K. In contrast, the mean $\Delta\theta$ was close to 0 K in the dry case. The distribution of $\Delta\theta$ between the upstream location and the crest is almost identical to the one between the upstream location and the lower Rhine valley, i.e., most diabatic temperature changes occur upstream of the Alpine crest. This would be consistent with a major contribution of latent heating during cloud and precipitation formation in the main ascent region over the southern slopes, which will be further explored below. Trajectories at high downstream altitudes have on average larger absolute $\Delta\theta$ than trajectories passing through the Rhine valley (Fig. 11a and c). For the latter, $\Delta\theta$ values are even predominantly negative between 00–06 UTC on 15 May and between 18 UTC 15 May and 03 UTC 16 May. A comparison of Fig. 11a and Fig. 11b shows that (i) trajectories passing through the Rhine valley have a larger ΔT and a smaller $\Delta\theta$ than trajectories passing aloft and (ii) ΔT and $\Delta\theta$ are anti-correlated particularly in the second half of the foehn event. As discussed in more detail later, this is explicable by a larger positive vertical displacement of trajectories experiencing latent heating and smaller positive or negative vertical displacement of trajectories experiencing latent cooling.

Specific moisture changes Δq along trajectories are much larger than in the dry case: values vary between -7.7 $\mathrm{g kg}^{-1}$ and 4.7 $\mathrm{g kg}^{-1}$. About 67 % of trajectories lose moisture during the passage of the Alpine crest (Fig. 11b). Moisture losses occur predominantly along trajectories passing the Rhine valley at higher altitudes, while the majority of trajectories passing through the Rhine valley gain moisture almost during the entire foehn event. Higher-level trajectories appear to have small moisture losses between 9–18 UTC on 15 May (Fig. 11a and c). However, as indicated by Fig. 11c, altitudes above 4.5 km are not sampled by the trajectories during the latter time period. At other times the majority of the trajectories in this altitude range were losing moisture. Similarly to $\Delta\theta$, Δq over the northern slope is generally very small as indicated by the similarity of the two histograms in Fig. 12b. This further supports the importance of precipitation formation for the diabatic temperature changes.

The temperature change due to cloud microphysical processes can be calculated according to eq. 3. Based on this estimate latent heating explains on average 58.7 % of the total diabatic temperature change. However, the explained fraction varies strongly with time: latent heating is least important during the morning and early afternoon of 15 May (explained variance smaller than 40 %), while at other times it explains a large fraction of $\Delta\theta$ (up to 90 % on 16 May). Latent heating contributions are also more important for trajectories with downstream altitudes larger than 1.7 km. Trajectories passing through the valley atmosphere are more likely affected by turbulent mixing, which may explain the smaller contribution of latent heating. Consistent with this hypothesis, the diabatic temperature changes on the downstream side are larger for these trajectories compared to those passing above the valley atmosphere (not shown). The remaining unattributed potential temperature change (10–60 % of the total) suggests that radiative and mixing processes play an important role in the potential temperature budget, which was also the case in the dry foehn event. Fig. 14 shows this residual potential temperature change ($\Delta\theta - S_{lh}$). Compared to $\Delta\theta$ the residual temperature changes are more evenly distributed with altitude and show a clear diurnal cycle with larger values during daytime. Overall, the structure of the residual temperature changes

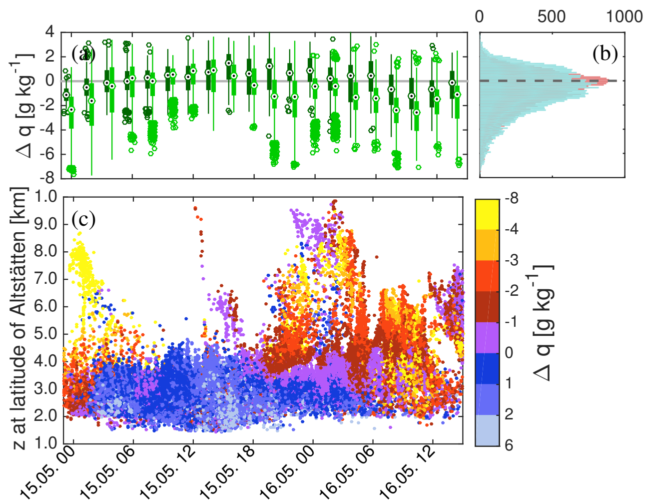

Figure 12. Moist foehn case: specific moisture change Δq along trajectories between their upstream location and Altstätten (see definitions in Fig. 3). (a, b) are identical to those in Fig. 6 but pertain to specific moisture content. (c) Each dot corresponds to a trajectory passing above 47.4°N at the corresponding time and altitude. The color coding corresponds to the Δq between the upstream location and Altstätten.

closely resembles the one of $\Delta\theta$ in the dry case, albeit with slightly larger absolute values.

Further insight into the role of microphysical processes on the potential temperature budget can be gained by assessing the contribution of individual microphysical processes to the overall latent heating. Relevant microphysical processes are condensation of liquid water, evaporation of liquid water, freezing of liquid water to solid particles including riming, melting of solid particles to liquid drops, deposition of water vapour on solid particles and sublimation of solid particles. The latent heating rates for each of these processes were calculated by integrating equation 3 along each trajectory. Fig. 13 shows the evolution of these terms for trajectories passing the Rhine valley at different height intervals. Although the contribution of individual processes varies throughout the foehn event, some general patterns can be identified. Latent heating by condensation, deposition and freezing is most important for parcels with downstream altitudes larger than 3 km (Fig. 13b and d). Processes associated with latent cooling are insignificant. In contrast, sublimation, melting and evaporation are important for trajectories arriving at lower altitudes and condensation, deposition and freezing are insignificant except for the last 18 h of the foehn event (Fig. 13a and c). For parcels below 1.5 km latent cooling even dominates the total potential temperature change around 00 UTC on 16 May (Fig. 13a).

The transition from the dominance of latent heating to a stronger contribution from latent cooling with decreasing arrival altitude in the Rhine valley is very interesting in terms of foehn flow dynamics. Parcels experiencing strong latent heating during the ascent may be too buoyant to descend into the northern Alpine foehn valleys, while parcels primarily influenced by evaporation, sublimation and melting may descend more easily on the leeward side. The potential role of latent cooling in the descent of foehn air into the valley is also interesting from a model perspective, since, in particular, the melting of snow and graupel is typically not very well represented in microphysical schemes (e.g., Frick *et al.* 2013).

5. Conclusions

Foehn air warming is investigated for two different south foehn events in the northern Alpine Rhine valley. One event is characterised by barely any precipitation on the Alpine south side during its first phase (4-7 March 2013, dry foehn event). Strong upstream precipitation occurs in the second case (14-16 May 2013, moist foehn event). The analysis relies on trajectories which are calculated from COSMO-model wind fields with a grid spacing of 2 km and a temporal resolution of 20 s. Additionally, a multitude of thermodynamic and microphysical parameters are traced along trajectories, which in turn allows the warming due to isentropic drawdown and microphysical processes to be quantified. Warming due to turbulent mixing and radiative processes is, however, only qualitatively assessed.

The Lagrangian analysis allows us to draw the following main conclusions with respect to the research questions posed at the end of the introduction:

1. In both cases, a fairly complicated flow pattern with several distinct air streams upstream of the Alps occurs. This is consistent with earlier results from Rotunno and Ferreti (2003). While in the dry case most foehn air parcels originate at upstream altitudes above 1.5 km, low-level parcels originating close to sea level contribute strongly to the foehn flow in the moist case. Trajectories in the dry case rise only slightly during the upstream approach of the Alps and then rapidly descend into the foehn valley (mean vertical displacement 700 m). In contrast, trajectories in the moist foehn case ascend rapidly over the southern slope, but only 50 % of the trajectories finally descend into the foehn valley.
2. In both cases, a large fraction of the temperature change can be attributed to adiabatic processes, which explain 79 % and 70 % of the temperature variance, respectively. Accordingly, isentropic drawdown is the key warming mechanism. In the moist foehn case, latent heating and cooling account for 58.7 % of the variance in potential temperature. The spatio-temporal distribution of the potential temperature changes in the dry foehn case suggests an important role for turbulent mixing with boundary layer air, which itself is affected by radiative heating during daytime and radiative cooling during night time. Additionally, internal mixing of the foehn air mass may result in diabatic temperature changes. In the moist foehn case, the potential temperature changes not attributable to moist processes exhibit a very similar spatio-temporal distribution, but have a slightly larger amplitude.
3. Moist processes played an important role for potential temperature changes in the moist foehn case. For parcels travelling through the Rhine valley at altitudes below 1.5 km, evaporation, sublimation and melting are the most important processes, i.e., processes associated with latent cooling. In contrast, condensation, deposition and freezing dominate for parcels arriving above 3 km, i.e., processes associated with latent heating. In this respect, the vertical "scrambling" of air parcels is an interesting aspect of our model simulations: Parcels producing a large amount of condensate during the upwind-side ascent are strongly warmed by latent heating and are, therefore, too buoyant to descend on the leeward side. In contrast, parcels passing below the cloud layer or in the region of the melting layer are cooled by evaporation, sublimation and melting, which leads to a small or even negative $\Delta\theta$. The latter, therefore, descend more readily into the Rhine valley. A schematic illustration of the vertical flow pattern is provided in Fig. 1c. Note that the depicted parcels will not have the same horizontal path on the upstream side, but will ascend at different longitudes. A vertical "scrambling" focussing on the positive buoyancy of air parcels generating the condensate has been previously hypothesised by Smith *et al.* (2003) based on a small trajectory sample for a

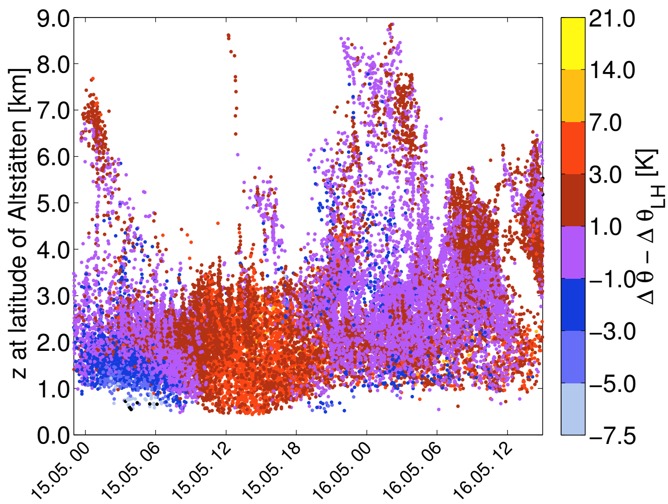

Figure 14. Moist foehn case: difference between the total potential temperature change between 45°N and 47.4°N and the potential temperature change due to latent heating (colour coding). Each dot corresponds to a trajectory passing above 47.4°N at the corresponding time and altitude during the May 2013 foehn event.

south foehn case. This hypothesis is clearly confirmed by our investigations. The importance of latent cooling for air parcels arriving close to the foehn valley floor has been indicated in a few earlier studies (e.g., Mayr *et al.* 2004), but is quantitatively assessed for the first time in this study.

Future studies should investigate the hypothesis of air parcel scrambling, the importance of latent cooling in other foehn events and address the implications for foehn air dynamics in more detail. It would also be important to perform a complete budget analysis of potential temperature and moisture along trajectories, as the conservation of these properties in the absence of diabatic processes is an important assumption in Lagrangian studies. In particular, a non-conservation of potential temperature along trajectories affects the "residual" potential temperature changes, i.e., related to radiative and mixing processes, and should therefore not strongly impact the major conclusions of this paper.

Acknowledgements

The work presented in this paper was partly funded by ETH research grant ETH-38 11-1. We acknowledge the AGF for their help with selecting the case studies. We thank Robin Stevens and Dan Grosvenor for proof-reading the manuscript and both reviewers for their helpful comments.

References

Arbeitsgemeinschaft Föhnforschung Rheintal-Bodensee. 2014. Föhndatenbank. *www.agf.ch* .

Baldauf M, Seifert A, Förstner J, Majewski D, Raschendorfer M. 2011. Operational convective-scale numerical weather prediction with the COSMO model: Description and sensitivities. *Mon. Wea. Rev.* **139**: 3887–3905, doi:10.1175/MWR-D-10-05013.1.

Batchelor GK. 1967. *An introduction to fluid dynamics*. Cambridge University Press.

Baumann K, Maurer H, Rau G, Piringer M, Pechinger U, Prevot A, et al. 2001. The influence of south foehn on the ozone distribution in the Alpine rhine valley – results from the MAP field phase. *Atmos. Environ.* **35(36)**: 6379–6390, doi:10.1016/S1352-2310(01)00364-8.

Bougeault P, Binder P, Buzzi A, Dirks R, Kuettner J, Houze R, Smith RB, Steinacker R, Volkert H. 2001. The MAP special observing period. *Bull. Amer. Meteor. Soc.* **82**: 433–462.

Bowman KP, Lin JC, Stohl A, Draxler R, Konopka P, Andrews A, Brunner D. 2013. Input data requirements for Lagrangian trajectory models. *Bull. Am. Meteorol. Soc.* **94**: 1051–1058, doi:10.1175/BAMS-D-12-00076.1.

Chen WD, Smith RB. 1987. Blocking and deflection of airflow by the Alps. *Mon. Wea. Rev.* **115**: 2578–2597.

Dee DP, Uppala SM, Simmons AJ, Berrisford P, Poli P, Kobayashi S, Andrae U, Balmaseda MA, Balsamo G, Bauer P, Bechtold P, Beljaars ACM, van de Berg L, Bidlot J, Bormann N, Delsol C, Dragani R, Fuentes M, Geer AJ, Haimberger L, Healy SB, Hersbach H, Hólm EV, Isaksen L, Kållberg P, Köhler M, Matricardi M, McNally AP, Monge-Sanz BM, Morcrette JJ, Park BK, Peubey C, de Rosnay P, Tavolato C, Thépaut JN, Vitart F. 2011. The ERA-Interim reanalysis: configuration and performance of the data assimilation system. *Q. J. R. Meteorol. Soc.* **137**: 553–597, doi: 10.1002/qj.828.

Dove HW. 1867. *über eiszeit, föhn und scirocco*. 116pp, Reimer Berlin.

Doyle JD, Epifanio CC, Persson A, Reinecke PA, Zängl G. 2013. Mesoscale modeling over complex terrain: numerical and predictability perspectives. In: *Mountain Weather Research and Forecasting*, vol. 219, Chow K, Wekker SD, Snyder B (eds), Springer Atmos. Sci., pp. 531–589. 750 pp.

Drobinski P, Steinacker R, Richner H, Baumann-Stanzer K, Beffrey G, Benech N, Berger H, Chimani B, Dabas A, Dorninger M, Dürr B, Flamant C, Frioude M, Furger M, Gröhn I, Gubser S, Gutermann T, Häberli C, Häller-Scharnhost E, Jaubert G, Lothon M, Mitev V, Pechinger U, Ratheiser M, Ruffieux D, Seiz G, Spatzierer M, Tschannett S, Vogt S, Werner R, Zängl G. 2007. Föhn in the rhine valley during map: A review of its multiscale dynamics in complex valley geometry review of its multiscale dynamics in complex valley geometry. *Q. J. R. Meteorol. Soc.* **133**: 897–916, doi: 10.1002/qj.70.

Elvidge AD, Renfrew IA. 2015. The causes of foehn warming in the lee of mountains. *Bull. Amer. Meteor. Soc* **in press**, doi:10.1175/ BAMS-D-14-00194.1.

Elvidge AD, Renfrew IA, King JC, Orr A, Lachlan-Cope TA. 2014. Foehn warming distributions in nonlinear and linear flow regimes: a focus on the antarctic peninsula. *Q. J. R. Meteorol. Soc.* doi:10.1002/qj.2489.

Elvidge AD, Renfrew IA, King JC, Orr A, Lachlan-Cope TA, Weeks M, Gray SL. 2015. Foehn jets over the Larsen C ice shelf, Antarctica. *Q. J. R. Meteorol. Soc.* **141**: 698–713.

Flamant C, Drobinski P, Furger M, b Chimani, Tschannett S, Steinacker R, Protat A, Richner H, Gubser S, Häberli C. 2006. Föhn/cold-pool interactions in the Rhine valley during MAP IOP 15. *Q. J. R. Meteorol. Soc.* **132**: 3035–3058, doi:10.1256/qj.06.36.

Frick C, Seifert A, Wernli H. 2013. A bulk parameterization of melting snowflakes with explicit liquid water fraction for the cosmo model. *Geoscientific Model Development* **6**(2): 1925–1939, doi:10.5194/ gmd-6-1925-2013.

Gohm A, Mayr GJ, Fix A, Giez A. 2008. On the onset of bora and the formation of rotors and jumps near a mountain gap. *Q. J. R. Meteorol. Soc.* **134**: 21–46, doi:10.1002/qj.206.

Grell GA, Knoche R, Peckham SE, McKeen SA. 2004. Online versus offline air quality modeling on cloud-resolving scales. *Geophys. Res. Lett.* **31**: L16 117, doi:10.1029/2004GL020175.

Grosvenor DP, King JC, Choularton TW, Lachlan-Cope T. 2014. Downslope föhn winds over the Antarctic Peninsula and their effect on the Larsen Ice Shelves. *Atmos. Chem. Phys.* **14**: 9481–9509, doi:10.5194/ acp-14-9481-2014.

Hann J. 1866. Zur Frage über den Ursprung des Föhns. *Zeitschrift der österreichischen Gesellschaft für Meteorologie* : 257–263.

Hann J. 1885. Einige Bemerkungen zur Entwickelungs-Geschichte der Ansichten über den Ursprung des Föhn. *Meteorol. Z.* **2**: 393–399. English translation by Volken/Brönnimann in Meteor. Z., 21 (2012), 591-596.

Heer O, von der Linth AE. 1852. *Zwei geologische vorträge, gehalten im märz 1852*. Zürich.

Ishizaki N, Takayabu I. 2009. On the warming events over Toyama Plain by using NHRCM. *SOLA* **5**: 129–132, doi:10.2151/sola.2009-033.

Kljun N, Sprenger M, Schär C. 2001. Frontal modification and lee cyclogenesis in the Alps: a case case study using the alpex reanalysis data set. *Meteorol. Atmos. Phys.* **78**: 89 105.

Mayr GJ, Armi L, Arnold S, Banta RM, Darby LS, Durran DD, Flamant C, Gabersek S, Gohm A, Mayr R, Mobbs S, Nance LB, Vergeiner I, Vergeiner J, Whiteman CD. 2004. Gap flow measurements during the Mesoscale Alpine Programme. *Meteorol. Atmos. Phys.* **86**: 99–119.

Miltenberger AK. 2014. Lagrangian perspective on dynamic and micro-physical processes in orographically forced flows. PhD thesis, Diss. Eid-genössische Technische Hochschule ETH Zürich, Nr. 22227, doi:10.3929/ ethz-a-010406950.

Miltenberger AK, Pfahl S, Wernli H. 2013. An online trajectory module (version 1.0) for the non-hydrostatic numerical weather prediction model COSMO. *Geosci. Model Dev.* **6**: 1989–2004, doi:10.5194/ gmd-6-1989-2013.

Miltenberger AK, Seifert A, Joos H, Wernli H. 2015. A scaling relation for warmphase orographic precipitation: a Lagrangian analysis for 2D mountains. *Q. J. R. Meteorol. Soc.* doi:10.1002/qj.2514.

Olafsson H. 2005. The heat source of the foehn. *Hrvatski Meteoroloski Casopis* **40**: 542–545.

Raschendorfer M. 2001. The new turbulence parameterization of lm. *COSMO Newsletter* **1**: 89–97.

Richner H, Baumann-Stanzer K, Benech B, Berger H, Chimani B, Dorninger M, et al. 2006. Unstationary aspects of foehn in a large valley. Part I: operational setup, scientific objectives and analysis of the cases during the special observing period of the MAP subprogramme FORM. *Meteorol. Atmos. Phys.* **92**: 255–284, doi:10.1007/s00703-005-0134-y.

Richner H, Hächler P. 2013. Understanding and forecasting alpine foehn. In: *Mountain Weather Research and Forecasting*, vol. 219, Chow K, Wekker SD, Snyder B (eds), Springer Atmos. Sci., pp. 219–260. 750 pp.

Roch A. 2011. Orographic blocking in the alps: a climatological lagrangian study. Master thesis, ETH Zurich, available at URL www.iac.ethz.ch/groups/wernli.

Rotunno R, Ferreti R. 2003. Orographic effects on rainfall in MAP cases IOP 2b and IOP 8. *Q. J. R. Meteorol. Soc.* **129**: 373–390, doi:10.1256/qj.02.20.

Seibert P. 1990. South foehn studies since the ALPEX experiment. *Meteorol. Atmos. Phys.* **43**: 91–103.

Seibert P. 2004. Hann's thermodynamic foehn theory and its presentation in meteorological textbooks in the course of time. *Proc. ICHM, Polling* : 6 pAvailable at http://www.meteohistory.org/2004polling_preprints.

Seibert P. 2005. Hann's thermodynamic foehn theory and its presentation in meteorological textbooks in the course of time. *From Beaufort to Bjerknes and Beyond, Algorismus* **52**: 169–180.

Seibert P, Feldmann H, Neininger B, Bäumle M, Trickl T. 2000. South foehn and ozone in the Eastern Alps - case study and climatological aspects. *Atmos. Environ.* **34**: 139–1394.

Seifert A, Beheng KD. 2006. A two-moment cloud microphysics parameterization for mixed-phase clouds. Part 1: model description. *Meteorol. Atmos. Phys.* **92**: 45–66, doi:10.1007/s00703-005-0112-4.

Smith RB, Jiang Q, Fearon MG, Tabary P, Dorninger M, Doyle JD, Benoit R. 2003. Orographic precipitation and air mass transformation: an Alpine example. *Q. J. R. Meteorol. Soc.* **129**: 433–454, doi:10.1256/qj.01.212.

Sodemann H, Schwierz C, Wernli H. 2008. Interannual variability of greenland winter precipitation sources: Lagrangian moisture diagnostic and north atlantic oscillation influence. *J. Geophys. Res.* **113**, doi:10.1029/2007JD008503.

Steinacker R. 2006. Alpiner Föhn – eine neue Strophe zu einem alten Lied. *Promet* **32**: 3–10.

Stevens B, Feingold G, Cotton WR, Walko RL. 1996. Elements of the microphysical structure of numerically simulated nonprecipitating stratocumulus. *J. Atmos. Sci.* **53**: 980–1006.

Stohl A, Seibert P. 1998. Accuracy of trajectories as determined from the conservation of meteorological tracers. *Q. J. R. Meteorol. Soc.* **124**: 1465–1484.

Takane Y, Kusaka H. 2011. Formation mechanisms of the extreme high surface air temperature of 40.9°c observed in the Tokyo metropolitan area: considerations of dynamic foehn and foehnlike wind. *J. Appl. Meteor. Climatol.* **50**: 1827–1841, doi:10.1175/JAMC-D-10-05032.1.

Vogt S, Jaubert G. 2004. Foehn in the Rhine Valley as seen by a wind-profiler-RASS system and comparison with the nonhydrostatic model Meso-NH. *Meteorol. Z.* **13**: 165–174, doi:10.1127/0941-2948/2004/0013-0165.

Wilhelm M. 2012. COSMO-2 model performance in forecasting foehn: a systematic process-oriented verification. Scientific Report 89, MeteoSchweiz.

Würsch M, Sprenger M. 2015. Swiss and Austrian foehn revisited: a Lagrangian-based analysis. *Meteorol. Z.* doi:10.1127/metz/2015/0647.

Zängl G, Chimani B, Häberli C. 2004. Numerical simulations of the foehn in the Rhine valley on 24 October 1999. *Mon. Wea. Rev.* **132**: 368–389, doi:10.1175/1520-0493(2004)132⟨0368:NSOTFI⟩2.0.CO;2.